Research Square

Preprints are preliminary reports that have not undergone peer review.
They should not be considered conclusive, used to inform clinical practice,
or referenced by the media as validated information.

Role of Subjacent Plasmon Layer in Improving Photoelectrochemical Response of Metal Oxide Photoelectrodes

Anupam Srivastav
Dayalbagh Educational Institute
Neeraj Kumar Biswas
Dayalbagh Educational Institute
Sakshi Saxena
Dayalbagh Educational Institute
Anuradha Verma
Dayalbagh Educational Institute
Abhishek Srivastava
GLA University
Sahab Dass (drsahabdas@gmail.com)
Dayalbagh Educational Institute

Research Article

Keywords: Plasmon, Photoelectrochemical water splitting, Sputtering, Surface plasmon resonance, Sol-gel

Posted Date: May 13th, 2022

DOI: https://doi.org/10.21203/rs.3.rs-1621395/v1

License: This work is licensed under a Creative Commons Attribution 4.0 International License.
Read Full License

Abstract

This report brings out the role of Au plasmons as the subjacent layer below TiO_2 in PEC water splitting for hydrogen generation. Au was deposited on an ITO sheet using DC sputtering with 5 nm and 20 nm thickness and annealed at 300^oC for 20 minutes in the N_2 atmosphere. TiO_2 in the form of the thin film was coated on the already deposited Au layer using a sol-gel spin coating method. Thin films were characterized using tools such as X-ray diffraction, scanning electron microscopy, energy dispersive X-ray spectroscopy, and optical absorption spectroscopy. The presence of Au as the subjacent layer in TiO_2 shows enhanced absorption (visible region) due to the plasmonic properties displayed by Au nanoparticles. TiO_2 with subjacent Au layer (5 nm thickness) was found to exhibit eight times higher photoresponse than the pristine sample at 1.0 V/SCE which can be ascribed to the plasmonic effect of gold nanoparticles extending absorption in the visible region of sunlight.

Introduction

Global development in any society is based on demand and supply of energy. It has been realized that existing sources of energy derived from fossil fuels are limited will not be able to fulfill the increasing demand for future generations. Apart from that, decarburizing our energy sources is also an important issue because their continuous use creates well-known hazards that threaten human health and are associated with global climate change, and are posing a great danger for our environment and eventually for the life on our planet (Vayssieres, 2009). World over innovations on finding sustainable and green alternate sources of energy are ongoing relentlessly to reach the level of generating “zero-carbon fuel Hydrogen”. Hydrogen has emerged out as one of the most promising energy carriers in recent times and also gaining increasing attention from the scientific community by virtue of its potency as efficient and carbon-neutral fuel of the future (Joy et al. 2018, Walter et al. 2010, Watanabe et al 2020, Palmer et al. 2020, Dawood et al. 2020).

Photoelectrochemical (PEC) technology is an ideal and promising way to produce hydrogen along with oxygen by harnessing solar energy from water splitting. Scientists world over are pursuing research on the design and synthesis of the most efficient electrode with characteristics like optical function for maximal absorption of solar energy, bandgap lying between 1.6-2.0 eV, corrosion resistance, straddling band edges with H_2O redox potentials, long lifetime of charge carriers, long-term stability in aqueous electrolyte, etc. but so far all these desired characteristic has not been achieved in a single semiconductor(Choudhary et al. 2012).

TiO_2 has been extensively explored for its application in hydrogen generation via photoelectrochemical and photocatalytic pathways referring to its properties like economic viability, environmentally friendly, stability, non-corrosive nature, abundance, etc (Hashimato et al. 2005, Naseri et al. 2010). Owing to a high bandgap of 3.2 eV, TiO_2 absorbs primarily the ultraviolet portion of the solar spectrum and limits its use in the visible spectrum. To enhance its absorption in the visible region various modifications have been

adopted like doping, dye sensitization, ion implantation, surface modification, the formation of composite system with other materials including plasmonic nanoparticles (Choi 2006, Subramanyam et al. 2020, Cao et al. 2020).

There are many reports which confirm that the presence of Au nanoparticles enhances the light absorption capability of TiO_2 (Cheng et al. 2020, Barczuk et al. 2020, Li et al. 2014, Nguyen et al. 2021, Abed et al. 2021, Atabaev 2021). Das (2020) sensitized TiO_2 with Au nanoparticles with their different concentrations (0.5-1 wt.%) and obtained the highest photocurrent of 10 μA cm^{-2} with 0.7 wt.%. The presence of Au nanoparticles enabled their photoactivity in the visible region. Xu (2017) obtained 2500 μA cm^{-2} photocurrent density on modifying the nanorod array of TiO_2 with Au nanoparticles at 1.23V vs. RHE on account of increased charge carrier density and light absorption due to plasmonic Au nanoparticles. F. Su (2013) attached plasmonic gold nanoparticles on the branched nanorod array of TiO_2 and obtained photocurrent of 125 μA cm^{-2} under visible light (≥ 420 nm). Due to plasmonic Au nanoparticles, enhancement in light absorption was found as well as promoted charge carrier separation and mobility. Zhan (2014) investigated two different configurations of TiO_2 viz. Au embedded in TiO_2 and Au sitting on TiO_2. They found that Au embedded in TiO_2 outperforms in light absorption and photocatalytic response.Naik(2019) reported high photocatalytic activity in nitrogen-doped Au@TiO_2 core-shell structures fabricated by the hydrothermal method. A hydrogen evolution rate of 4800 μmol per gram per hour was achieved under xenon light irradiation for a time duration of 240 min. The N doping does not bring crystallinity changes in TiO_2 while due to plasmonic Au impurity band is created between the valence band and conduction band of TiO_2. The localized surface plasmon resonance band demonstrated by gold nanoparticles present in the core was found to be responsible for reduced electron-hole pair recombination rate. Theoretical simulations by Gelle (2017) have revealed that a more intense local electrical field is created within the semiconductor near plasmonic metal nanoparticles in Au in TiO_2 configuration in comparison to Au on TiO_2 systems. Thus, an increase in segregation of charge carriers and extended visible light absorption is feasible in plasmonic Au nanoparticles embedded in the semiconductor matrix. High water splitting efficiency of amorphous black TiO_2 was reported by Shi (2018) on the use of plasmonic Au nanoparticles which resulted in photocurrent density of 2.82 mA/cm^2 at 1.23 V vs RHE which is significantly higher than unmodified photoelectrode of Au-TiO_2. The intermediate energy level in amorphous black TiO_2 improves the charge carrier separation resulting in high photoresponse. Mataresse (2019) designed hierarchial Au/TiO_2 nanostructures in different configurations viz. Au nanoparticles (NPs) as a bottom layer, top layer as well as in integrated assemblies for their application in water splitting and bisphenol A oxidation. They depicted the critical role of Au nanoparticles present at the bottom layer in exploiting the radiations through scattering effect and in turn the photoactivity of TiO_2. J. Jun (2019) fabricated a large-area 3D moth-eye Au NP/TiO_2/Au hierarchical structure by direct printing method and deposition process which showed 2–3 times high photocurrent density in comparison to 2D Au NP/TiO_2/Au absorber in the visible region. Atef (2021)investigated the tuning of Au nanoparticles deposited by a sputtering method on titania nanotube arrays exhibiting high

surface area. Au nanoparticles with an optimized diameter of 7–25 nm were distributed on titania nanotube arrays by adjusting the sputtering current. A computational study confirmed the redshift on account of localized surface plasmon resonance exhibited by Au nanoparticles. An eighty-six percent increase in photocurrent was observed in comparison to bare titania nanotube arrays. Liu (2021) fabricated ZnS-PbS quantum dot loaded Au/TiO_2 photocatalysts and obtained absorption from UV to infrared region. The extended absorption reduced charge recombination and hydrogen production rate of 5011 μmol $g^{-1}h^{-1}$ was achieved in the presence of a sacrificial reagent. An increase in hydrogen production rate by virtue of enhanced charge separation and conductivity has been demonstrated in ternary CdS/Au/TiO_2 photoanodes by Zhang et al(2021). A photocurrent of 2.78 mA/cm^2 at 1.23 V vs RHE was achieved which was approximately over twice more than the pristine sample. Verma et al (2016) reported the influence of irradiation by low energy ion beams on Au/TiO_2 thin films. Six times enhancement in photocurrent density was achieved compared with pristine sample on account of the reduced bandgap, charge transfer resistance, and higher value of V_{oc} (open-circuit voltage).

The investigation on the role of depositing Au nanoparticles of different thicknesses by a sputtering method as a subjacent layer below TiO_2 and its effect on the photoelectrochemical response has not been done so far to the best of our knowledge.

Experimental

Material and Methods:

The precursor Titanium tetraisopropoxide (TTIP) was procured from Sigma-Aldrich. Analytical grade ethanol and ethanolamine were also used to make the sol. Indium doped tin oxide (SnO_2:In) conducting glass substrate was obtained from SPI supplies, USA.

The schematic presentation of thin film preparation is shown below in Fig. 1.

Sputter coating of Au:

Gold sputter coater system available at IUAC, New Delhi (Quoram Technologies) was used to deposit Au on the cleaned one-third area of ITO glass substrate. The chamber pressure of 0.02 millibar of Argon was maintained to deposit 5 nm and 20 nm thick film and deposition was done for a duration of 30 s. Dry N_2 atmosphere for 20 mins at 300^0C was provided to anneal the prepared Au thin films.

Preparation of TiO_2 sol:

By mixing 3 mL TTIP in 2 mL of ethanolamine and 20 mL of ethanol, yellowish gel solution was obtained and used further to prepare titanium dioxide thin films. Reaction kinetics between ethanolamine and TTIP was enhanced by stirring the solution for 2 h at room temperature. Now over the plane ITO (for pristine sample) and Au thin films prepared in step 1 (See Fig. 1) (for TiO_2 with Au as a subjacent layer), obtained

gel solution was coated uniformly by putting 10 µL solution which was spin-coated at 2500 rotation per minute. Optimized results after repeated experimentation with plane TiO_2 were achieved with 6 layers deposition and therefore successively 6 layers were deposited over the planeITO and Au thin films. After deposition of each layer, films were kept for drying at a hot plate maintained at a temperature of 80^oC for 10 mins. The films thus obtained were kept for 2 h annealing at 450^oC in a muffle furnace (Step 2 and 3, Fig. 1.).

Preparation of electrodes:

All the annealed thin films of pristine and modified TiO_2 were converted into photoelectrodes with an effective surface area of a one-centimeter square for their use in a photoelectrochemical cell by adopting the method reported by Verma et al (2016).

Thin Films Characterization and Photoelectrochemical Measurements:

The obtained thin films were characterized for crystalline phase by the X-ray diffraction study using Cu Kα radiation source of λ = 1.5418Å with X-ray powder diffractometer (Bruker AXS, Model: D8 Advanced). The crystallite size was calculated using Scherrer's formula

$$D = 0.9\lambda/\beta\cos\theta$$

where λ is the wavelength of X-ray (1.54 Å),$\beta$is the full width at half maximum (FWHM), $\theta$is the Bragg's diffraction angle.

The UV- visible absorbance spectra (absorbance vs. wavelength) of TiO_2/Au thin films was obtained using Shimadzu, UV-2450, Japan UV–Visible Spectrophotometer. FE-SEM study was carried out using Carl Zeiss SUPRA 40VP system and EDS maps were obtained from MIRA II LMH (TESCAN).

In the PEC cell, three electrodes (Au/TiO_2: working; platinum mesh: counter and saturated calomel electrode (SCE): reference electrode) were immersed in 13 pH NaOH electrolyte solution. Current-voltage (I-V) characteristics of the electrodes were recorded under dark and light conditions using an Hg-Xe arc lamp (Oriel, USA) with100 mW cm^{-2} intensity and AM 1.5 G illumination. Applied bias was provided in a range of + 1.0 V/SCE to -1.0 V/SCE. The photocurrent density of photoelectrodes can be obtained by subtracting dark current (per square centimeter) from light current (per square centimeter). Mott–Schottky analysis was performed to obtain the flat band potential of the electrodes under dark conditions by varying potential from − 1 V/SCE to 1 V/SCE. Nyquist plots were also obtained to see the charge transfer properties by applying a bias of 1 V (vs SCE) with frequency and amplitude of 0.1 MHz–0.1 Hz and 10 mV respectively under illumination conditions.

Results And Discussion

XRD patterns obtained for the pristine TiO_2 (A)and with subjacent Au layer of thickness, 5nm (B) and 20nm (C) are presented in Fig. 2 (a). All films show peaks at 2θ = 25.28, 37.80, 48.04, 54.0 and 55.10 corresponding to the (101), (004), (200), (105) and (211) reflections confirming the formation of titanium dioxide with anatase phase of which matches with JCPDS card no. 21-1276 and for metallic Au, 2θ peaks were obtained at 38.18 and 44.392 corresponding to the (111) and (200) reflections which matches with JCPDS card no. 04-0784. The higher thickness of the 20 nm Au layer can be proved from the magnified view of (111) peak of Au showing higher intensity/counts in Fig. 2 (b).

The crystallite size of $TiO_2$and Au nanoparticles obtained by Scherrer's formula is as follows:

A) Plane TiO_2 – 19nm

B) TiO_2 with subjacent Au of 5 nm thickness- 16 nm with Au nanoparticles of ≅ 50 nm

C) TiO_2 with subjacent Au of 20 nm thickness- 17 nm with Au nanoparticles of ≅ 100 nm

The UV- Visible absorbance spectra (absorbance vs. wavelength) of the Au/TiO_2 thin films composite system is shown in Fig. 3.

The presence of the subjacent Au layer is responsible for visible light absorption by UV absorbing TiO_2. As can be seen from Fig. 3, 400 nm to 650 nm, plasmonic peaks due to Au nanoparticles are visible. As a consequence of plasmon resonance shown by Au nanoparticles improved absorption in the visible portion of sunlight was achieved (Ghobadi et al. 2020; Tudu et al. 2020). The reason for enhanced absorption in TiO_2 with 20 nm thickness Au subjacent layer is due to larger concentration in comparison to 5 nm thickness. Another reason may be assigned to the bigger particle size of Au nanoparticles in 20 nm thickness which has been confirmed by FESEM analysis. FESEM images are shown in Fig. 4 for Au thin films. Au film with 5nm thickness shows the uniform deposition of Au over the ITO substrate(Fig. 4(a))with a nanoparticles size of 40 to 50 nm while dense and agglomerated deposition of Au nanoparticles of bigger size (> 100 nm) is clearly perceptible in the case of 20 nm thickness Au film (Fig. 4 (b)) and the particle size corroborate with particle size obtained from Scherrer's equation. The EDS maps corresponding to Au thin films of 5 nm and 20 nm thickness shown in Fig. 4 (d-e) reveal that weight percentage is 4.2% and 12.3% respectively. The compact and dense deposition of titanium dioxide at the surface of Au nanoparticles is apparent in Fig. 4 (c) for TiO_2 with subjacent Au thin film of 5 nm thickness and the corresponding EDS map clearly shows the presence of Ti, O, and Au elements in Fig. 4 (f).

The photocurrent density of the electrodes is shown in Fig. 5 (a). The pristine TiO_2 exhibits the photocurrent density of 435 μA cm^{-2} under 1V/SCE bias condition while the TiO_2 with subjacent Au of 5 nm thickness showed approximately eight times enhanced photocurrent of 3348 μA cm^{-2} in comparison to pristine TiO_2. TiO_2 with subjacent Au of 20 nm thickness exhibits photocurrent density of 1309 μA cm^{-2} at 1V/SCE. In the case of a 5 nm thick Au subjacent layer, onset potential is also achieved earlier in

comparison to the other two samples. As can be seen from FESEM images shown in Fig. 4 (b) suggesting that annealing of sputtered Au film of 20 nm thickness resulted in agglomeration of Au nanoparticles with a size greater than 100 nm and such large-sized Au nanoparticles serve well as charge recombination centers. But the higher current in the case of TiO_2 with subjacent Au of 20 nm thickness in comparison to pristine $TiO_2$is due to Au nanoparticles of higher concentration which promote absorption in the visible region (Fig. 3) but reduced in comparison to 5 nm subjacent layer due to agglomerated Au nanoparticles in 20 nm thickness which acts as charge recombination center and reduces the photoelectrochemical performance (Sittishoktram et al. 2020). Thus, overall enhancement is due to the plasmonic effect of Au showing surface plasmon resonance (SPR) peak in the visible region of the solar spectrum i.e. 400–650 nm.

In addition to this, Mott-Schottky plots were obtained in dark conditions showing flat band potential of all electrodes. A more negative value of flat band potential (0.90 V/SCE) in TiO_2 with Au subjacent layer of 5 nm thickness confirms the reduced charge recombination rate. A positive value of the slope in MS curves demonstrates the n-type conductivity of the semiconductor thin films. Further, the Nyquist plots also confirm the least charge transfer resistance in the same sample and the findings corroborate with photocurrent density and flat band potential measurements.

Besides the role of Au nanoparticles in enhancing absorption of TiO_2 in visible light, the position of the conduction band of TiO_2 is above the Fermi level of Au which promotes the movement of charge carriers from TiO_2 to the subjacent Au layer and then towards the counter electrode through an external circuit in PEC cell to generate hydrogen (Verma et al, 2016).

Conclusions

A simple method has been chosen to deposit the titanium dioxide thin films on ITO using a sol-gel technique. Depositing Au using sputtering in the subjacent configuration is the novel way of studying the Au/TiO_2 composite system. To behave as plasmons, metal nanoparticle preparation is an important criterion as the properties of plasmon depend on their shape and size, and therefore the shift in surface plasmon resonance (SPR) peak also depends on these properties. In the present study, Au was deposited to increase the absorption of titanium dioxide in the visible portion of sunlight. Enhancement in the optical absorption in the visible region was observed and that also accounts for increased photoresponse of the Au/TiO_2 system. Higher photocurrent obtained in the case of subjacent Au with 5 nm thickness film has been supported by the flat band potential with more negative magnitude and reduced charge transfer resistance at the electrode-electrolyte interface.

Declarations

Authors Contribution

Anupam Srivastav: Conceptualization, Methodology, Writing- Original draft preparation, Investigation **Neeraj Kumar Biswas**: Visualization, Data Curation. **Sakshi Saxena**: Data curation, Editing, Formal analysis. **Anuradha Verma***:* Conceptualization, Visualization. **Abhishek Srivastava**: Software, Validation. **Sahab Dass:** Supervision, Research Activity Planning, Writing- Reviewing and Editing.

Acknowledgments

The author (s) would like to thank IUAC, New Delhi for FE-SEM characterization. We thank financial support by MNRE, Govt. of India under the project (103/241/2015-NT).

Funding Declaration

This work is supported under project (103/241/2015-NT) funded by MNRE, Govt. of India

Data Availability

The data used to support the findings of this study are included within the article and no additional source data are required.

Competing Interests Statement

The authors declare no financial and non-financial competing interests.

References

1. L. Vayssieres(2009)On Solar Hydrogen & Nanotechnology, John Wiley & Sons (Asia) Pte Ltd, Chap. 1.
2. Joy, J., Mathew, J. and George, S.C., (2018). Nanomaterials for photoelectrochemical water splitting–review. international journal of hydrogen energy, *43*(10): 4804–4817.
3. Walter, M. G., Warren, E. L., McKone, J. R., Boettcher, S. W., Mi, Q., Santori, E. A., & Lewis, N. S. (2010). Solar water splitting cells. Chemical Reviews, *110*(11): 6446–6473.
4. Watanabe, K., Iwase, A., & Kudo, A. (2020). Solar water splitting over Rh 0.5 Cr 1.5 O 3-loaded AgTaO 3 of a valence-band-controlled metal oxide photocatalyst. Chemical science, *11*(9): 2330–2334.
5. Palmer, G., & Floyd, J. (2020). Hydrogen as an energy carrier. In Energy Storage and Civilization,125–137.
6. Dawood, F., Anda, M., & Shafiullah, G. M. (2020). Hydrogen production for energy: An overview. International Journal of Hydrogen Energy45(7):3847–3869.
7. Choudhary, S., Upadhyay, S., Kumar, P., Singh, N., Satsangi, V.R., Shrivastav, R. and Dass, S., (2012) Nanostructured bilayered thin films in photoelectrochemical water splitting–A review. International journal of hydrogen energy, *37*(24): 18713–18730.
8. Hashimoto, K., Irie, H. and Fujishima, A., (2005) TiO_2 photocatalysis: a historical overview and future prospects. Japanese journal of applied physics, *44*(12R): 8269.

9. Naseri, N., Amiri, M. and Moshfegh, A.Z., (2010) Visible photoenhanced current–voltage characteristics of Au: TiO_2 nanocomposite thin films as photoanodes. Journal of Physics D: Applied Physics, *43*(10):105405.
10. Choi, W., 2006. Pure and modified TiO_2 photocatalysts and their environmental applications. Catalysis surveys from Asia, *10*(1): 16–28.
11. Subramanyam, P., Meena, B., Suryakala, D., Deepa, M. and Subrahmanyam, C., (2021) Plasmonic nanometal decorated photoanodes for efficient photoelectrochemical water splitting. Catalysis Today, 379:1–6.
12. Cao, Z., Yin, Y., Fu, P., Li, D., Zhou, Y., et al (2020). Branched TiO_2 Nanorod Arrays Decorated with Au Nanostructure for Plasmon-Enhanced Photoelectrochemical Water Splitting. Journal of The Electrochemical Society, 167(2): 026509.
13. Cheng, X., Dong, G., Zhang, Y., Feng, C., & Bi, Y. (2020). Dual-bonding interactions between MnO2 cocatalyst and TiO2 photoanodes for efficient solar water splitting. Applied Catalysis B: Environmental, 267: 118723.
14. Barczuk, P. J., Noworyta, K. R., Dolata, M., Jakubow-Piotrowska, K., &Augustynski, J. (2020). Visible-light activation of low-cost rutile TiO_2 photoanodes for photoelectrochemical water splitting. Solar Energy Materials and Solar Cells, 208: 110424.
15. Li, J., Cushing, S.K., Zheng, P., Senty, T., Meng, F. and Bristow, A.D., (2014). AyyakkannuManivannan, and Nianqiang Wu. Solar hydrogen generation by a CdS-Au-TiO_2 sandwich nanorod array enhanced with au nanoparticle as electron relay and plasmonic photosensitizer. J. Am. Chem. Soc., 136: 8438–8449.
16. Nguyen, T.T., Dao, K.A., Nguyen, T.T.O., Ung, T.D.T., Nguyen, D.T. and Nguyen, S.H., (2021). Unexpected impact of oxygen vacancies on photoelectrochemical performance of Au@ TiO_2 photoanodes. Materials Science in Semiconductor Processing, 127:105714.
17. Abed, J., Rajput, N.S., Moutaouakil, A.E. and Jouiad, M., (2020). Recent advances in the design of plasmonic Au/TiO_2 nanostructures for enhanced photocatalytic water splitting. Nanomaterials, 10(11): 2260.
18. Atabaev, T.S., (2018). Plasmon-enhanced solar water splitting with metal oxide nanostructures: a brief overview of recent trends. Frontiers of Materials Science, 12(3): 207–213.
19. Das, A., Dagar, P., Kumar, S., & Ganguli, A. K. (2020). Effect of Au nanoparticle loading on the photo-electrochemical response of Au–P25–TiO_2 catalysts. Journal of Solid State Chemistry, 281:121051.
20. Xu, F., Mei, J., Zheng, M., Bai, D., Wu, D., Gao, Z., & Jiang, K. (2017). Au nanoparticles modified branched TiO2 nanorod array arranged with ultrathin nanorods for enhanced photoelectrochemical water splitting. Journal of Alloys and Compounds, 693:1124–1132.
21. Su, F., Wang, T., Lv, R., Zhang, J., Zhang, P., Lu, J., & Gong, J. (2013). Dendritic Au/TiO_2 nanorod arrays for visible-light driven photoelectrochemical water splitting. Nanoscale, *5*(19): 9001–9009.

22. Zhan, Z., An, J., Zhang, H., Hansen, R. V., & Zheng, L. (2014). Three-dimensional plasmonic photoanodes based on Au-embedded TiO2 structures for enhanced visible-light water splitting. ACS applied materials & interfaces, *6*(2): 1139–1144.
23. Naik, G.K., Majhi, S.M., Jeong, K.U., Lee, I.H. and Yu, Y.T., (2019). Nitrogen doping on the core-shell structured Au@ TiO2 nanoparticles and its enhanced photocatalytic hydrogen evolution under visible light irradiation. Journal of Alloys and Compounds, 771:505–512.
24. Gellé, A. and Moores, A., (2017). Water splitting catalyzed by titanium dioxide decorated with plasmonic nanoparticles. Pure and Applied Chemistry, 89(12):1817–1827.
25. Shi, L., Li, Z., Dao, T.D., Nagao, T. and Yang, Y., 2018. A synergistic interaction between isolated Au nanoparticles and oxygen vacancies in an amorphous black TiO_2nanoporous film: toward enhanced photoelectrochemical water splitting. Journal of Materials Chemistry A, 6(27):12978–12984.
26. Matarrese, R., Mascia, M., Vacca, A., Mais, L., Usai, E.M., Ghidelli, M., Mascaretti, L., Bricchi, B.R., Russo, V., Casari, C.S. and Li Bassi, A., (2019). Integrated Au/TiO_2 nanostructured photoanodes for photoelectrochemical organics degradation. Catalysts, 9(4): 340.
27. Jun, J., Kim, H., Choi, H.J., Lee, T.W., Ju, S., Baik, J.M. and Lee, H., (2019). A large-area fabrication of moth-eye patterned Au/TiO2 gap-plasmon structure and its application to plasmonic solar water splitting. Solar Energy Materials and Solar Cells, 201: 110033.
28. Atef, N., Emara, S.S., Eissa, D.S., El-Sayed, A., Abdelraouf, O.A. and Allam, N.K., (2021). Well-dispersed Au nanoparticles prepared via magnetron sputtering on TiO_2 nanotubes with unprecedentedly high activity for water splitting. Electrochemical Science Advances, 2000004.
29. Liu, R., Fang, S.Y., Dong, C.D., Tsai, K.C. and Yang, W.D., (2021). Enhancing hydrogen evolution of water splitting under solar spectra using Au/TiO_2 heterojunction photocatalysts. International Journal of Hydrogen Energy, 46(56):28462–28473.
30. Zhang, T., Liu, C., Zhu, S., Zhang, C., Chen, X. and Chen, Z., (2021). Rational modulation for electron migration in CdS/Au/TiO_2 photoanode for efficient photoelectrochemical water oxidation. Inorganic Chemistry Communications, 129: 108625.
31. Verma, A., Srivastav, A., Sharma, D., Banerjee, A., Sharma, S., Satsangi, V.R., Shrivastav, R., Avasthi, D.K. and Dass, S., (2016) A study on the effect of low energy ion beam irradiation on Au/TiO2 system for its application in photoelectrochemical splitting of water. Nuclear Instruments and Methods in Physics Research Section B: Beam Interactions with Materials and Atoms, 379:255–261.
32. Ghobadi, T. G. U., Ghobadi, A., Soydan, M. C., Vishlaghi, M. B., Kaya, S., Karadas, F., &Ozbay, E. (2020). Strong Light-matter Interaction in Au Plasmonic Nanoantennas Coupled with Prussian Blue Catalyst on $BiVO_4$ for Photoelectrochemical Water Splitting. *ChemSusChem*.
33. Tudu, B., Bortamuly, R., &Saikia, P. (2020). Noble Materials for Photoelectrochemical Water Splitting. Photoelectrochemical Water Splitting: Materials and Applications, 71: 183.
34. Sittishoktram, M., Yaemsanguansak, P., Tuayjaroen, R., Asanithi, P., &Jutarosaga, T. (2020). Photoluminescence study of interfacial charge transfer and photocatalytic activity in titanium

dioxide/copper multilayer film. Materials Science in Semiconductor Processing, 108: 104886.

Figures

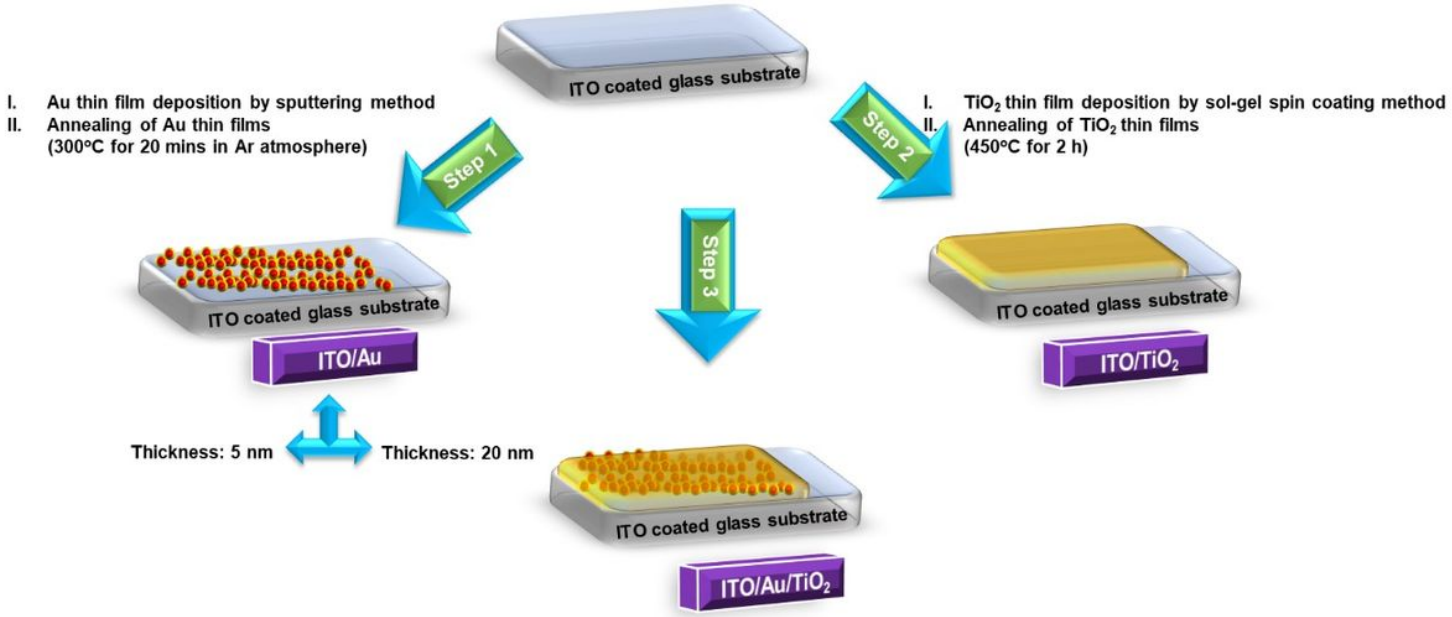

Figure 1

Schematic view of steps involved in thin film fabrication

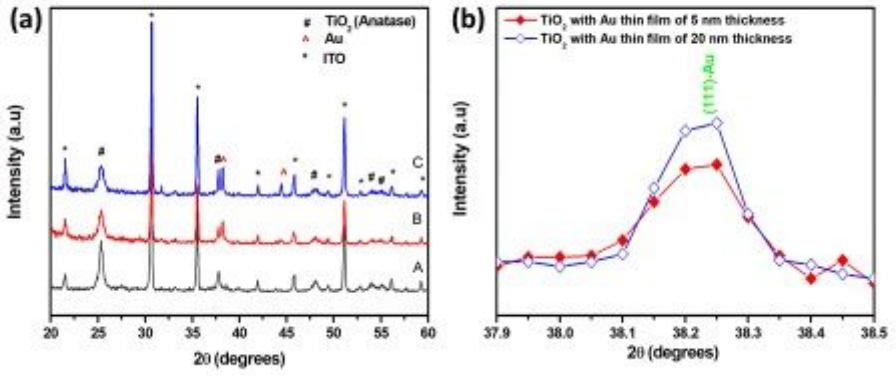

Figure 2

(a) X-ray Diffraction patterns of A) Pristine TiO_2 B) Subjacent Au thin film of 5 nm thickness and C) Subjacent Au thin film of 20 nm thickness (b) Enlarged view of (111) peak of Au

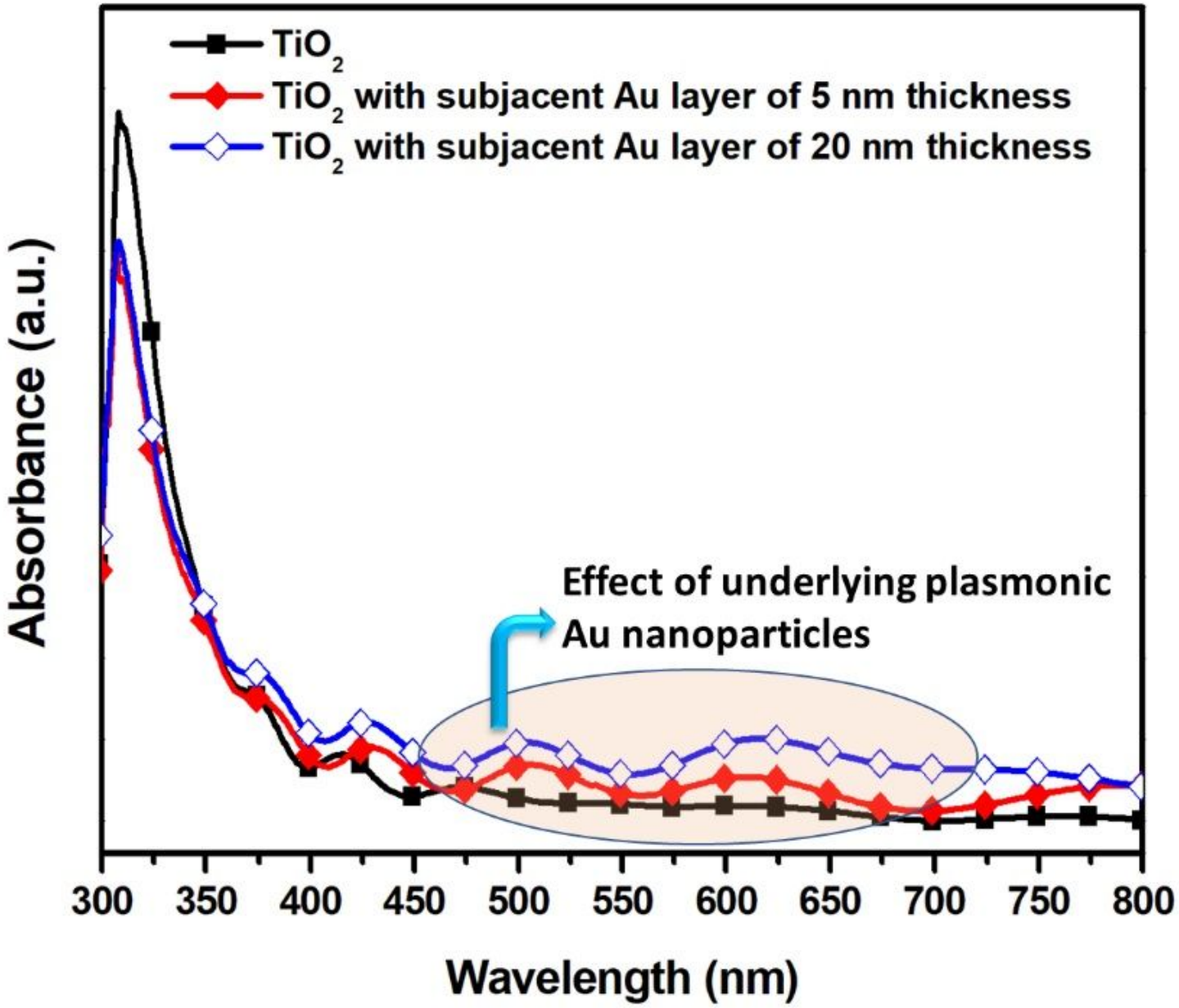

Figure 3

Absorption spectra of TiO_2 and TiO_2 with subjacent Au layer

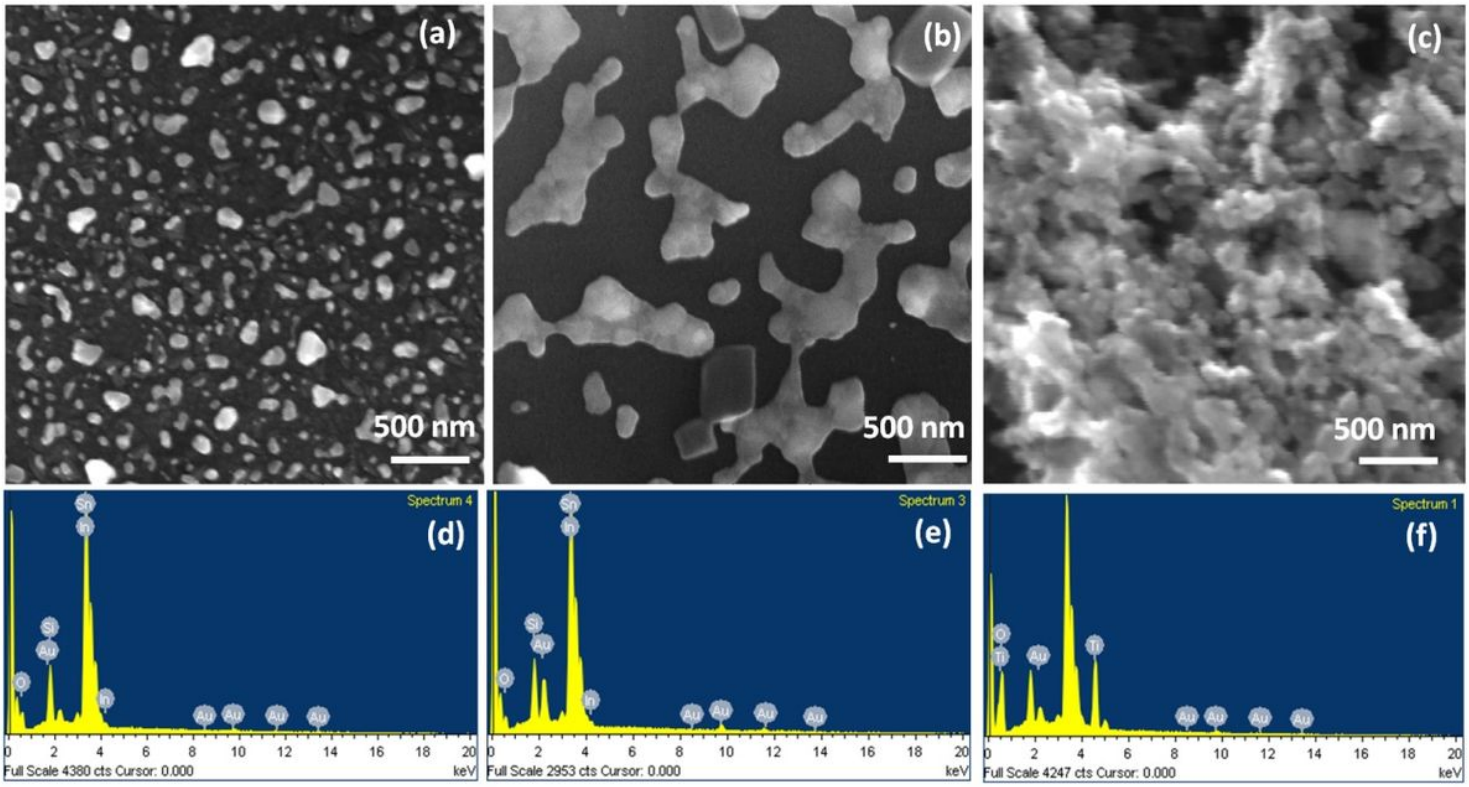

Figure 4

FESEMimage of a) Au-5 nm thickness b) 20 nm thickness c)TiO_2 with subjacent Au thin film of 5 nm thickness and EDAX maps of d) Au-5 nm thickness e) 20 nm thickness f)TiO_2 with subjacent Au thin film of 5 nm thickness

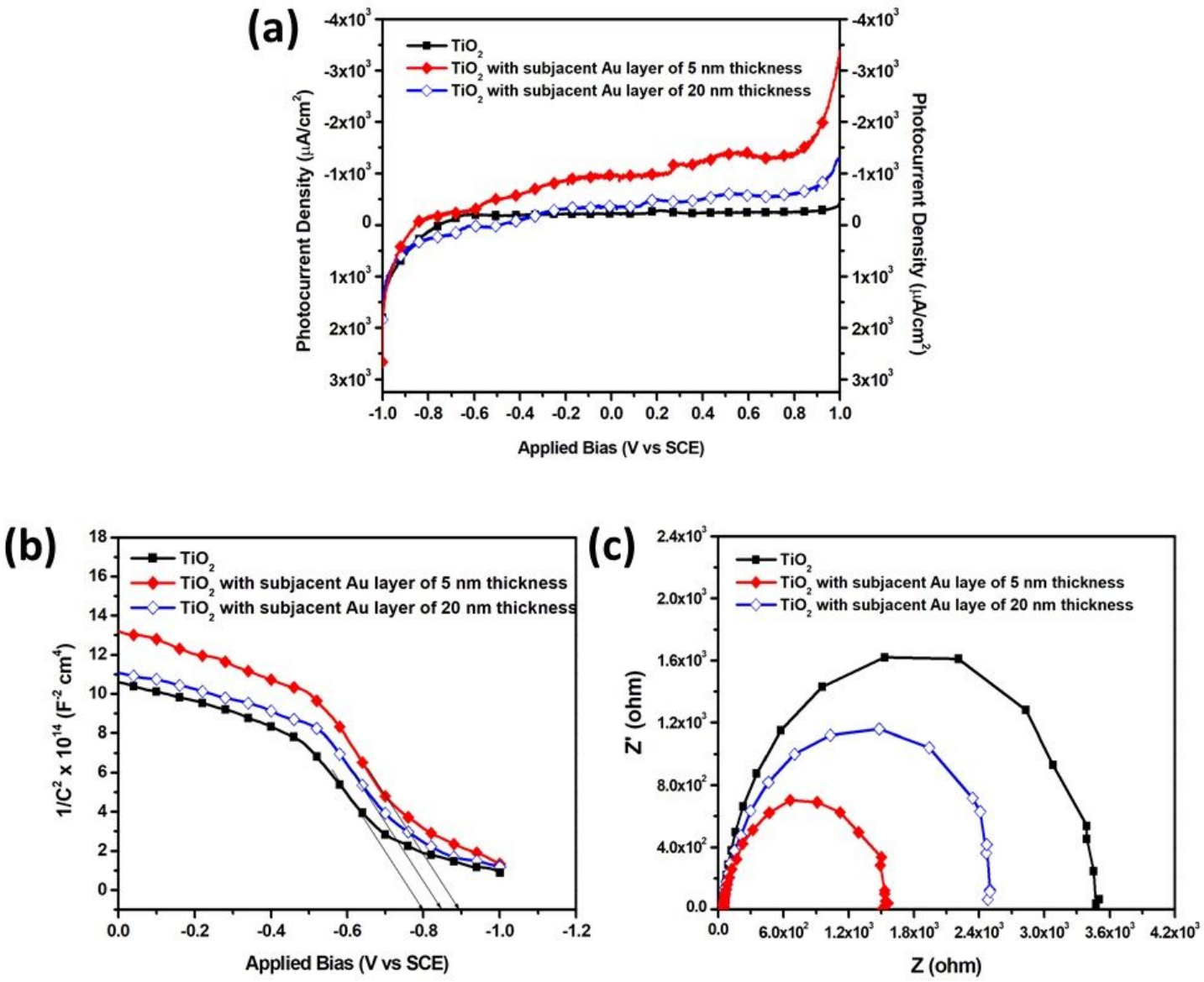

Figure 5

(a) Photocurrent density vs applied bias curves (b) Mott- Schottky plots (c) Nyquist plots for Plane TiO_2, and TiO_2 with subjacent Au layer of 5 nm and 20 nm thickness

Supplementary Files

This is a list of supplementary files associated with this preprint. Click to download.

- GraphicalAbstract.jpg